Nanoscale Res Lett (2010) 5:81–88
DOI 10.1007/s11671-009-9447-y

NANO EXPRESS

New Hybrid Properties of TiO_2 Nanoparticles Surface Modified With Catecholate Type Ligands

Ivana A. Janković · Zoran V. Šaponjić · Enis S. Džunuzović · Jovan M. Nedeljković

Received: 26 March 2009 / Accepted: 24 September 2009 / Published online: 13 October 2009
© to the authors 2009

Abstract Surface modification of nanocrystalline TiO_2 particles (45 Å) with bidentate benzene derivatives (catechol, pyrogallol, and gallic acid) was found to alter optical properties of nanoparticles. The formation of the inner-sphere charge–transfer complexes results in a red shift of the semiconductor absorption compared to unmodified nanocrystallites. The binding structures were investigated by using FTIR spectroscopy. The investigated ligands have the optimal geometry for chelating surface Ti atoms, resulting in ring coordination complexes (catecholate type of binuclear bidentate binding–bridging) thus restoring in six-coordinated octahedral geometry of surface Ti atoms. From the Benesi–Hildebrand plot, the stability constants at pH 2 of the order 10^3 M^{-1} have been determined.

Keywords TiO_2 nanoparticles · Surface modification · Catechol · Pyrogallol · Gallic acid

Introduction

The mechanism of semiconductor-assisted photocatalytic processes is based on the principle that colloidal semiconductor nanoparticles behave as miniature photoelectrochemical cells [1–3]. The overall photoexcitation process of semiconductor nanoparticles by ultra bandgap energies involve the photogeneration of electron–hole pairs within particle, followed by the competition between recombination, interfacial charge transfer to adsorbed compounds, and migration into midgap surface states [4].

Nanocrystalline TiO_2 has attracted widespread attention as a photocatalyst in various practical applications [5–7] as well as the part of photoelectrochemical systems, such as Grätzel cells [3]. Although nanoparticulate TiO_2 is very effective from an energetic point of view, it is a relatively inefficient photocatalyst. Due to its large bandgap ($E_g = 3.2$ eV), TiO_2 absorbs less than 5% of the available solar light photons. The main energy loss is due to the process of radiative or nonradiative recombination of charges generated upon photoexcitation of TiO_2, which is manifested as the relatively low efficiency of long-lived charge separation. Hence, the successful photochemical energy conversion and subsequent chemical reactions require both the extended separation of photogenerated charges and the response in the visible spectral region.

To achieve larger separation distances, preventing the hole–electron recombination before desired redox reaction occurs, reconstructed surface of TiO_2 nanoparticle surface was employed for establishing a strong coupling with electron-accepting and/or electron-donating species [8, 9]. Consequently, the lifetime of charge separation and photocatalytic activity of TiO_2 nanoparticles are increased. The origin of the unique photocatalytic activities of TiO_2 nanoparticles comparing to the bulk is found in larger surface area and the existence of surface sites with distorted coordination. Owing to large curvature of TiO_2 particles in the nanosize regime, the surface reconstructs in such manner that distorts the crystalline environment of surface Ti atoms forming coordinatively unsaturated Ti atoms. The changes in the pre-edge structure of Ti K-edge spectrum (XANES) of TiO_2 nanoparticles ($d < 20$ nm)

I. A. Janković (✉) · Z. V. Šaponjić · J. M. Nedeljković
Laboratory for Radiation Chemistry and Physics, Vinča Institute of Nuclear Sciences, P.O. Box 522, 11001 Belgrade, Serbia
e-mail: ivanaj@vinca.rs

E. S. Džunuzović
Faculty of Technology and Metallurgy, Department of Physical Chemistry and Electrochemistry, University of Belgrade, Karnegijeva 4, 11120 Belgrade, Serbia

revealed the existence of square–pyramidal coordination of surface Ti atoms (pentacoordinate) [10]. The results obtained from measurements of XAFS spectra of TiO_2 nanoparticles proved the existence of shorter Ti–O bond lengths (1.71 Å) as compared to bulk anatase TiO_2 (1.96 Å) [11]. The bond length distortion is also related to large curvature of nanometer size particles. These surface Ti atoms are very reactive and act as traps for photogenerated charges [12]. It was reported, on a whole class of electron-donating enediol ligands [9, 13], benzene derivatives [14], or mercapto-carboxylic acids [15] that binding to coordinatively unsaturated Ti atoms simultaneously adjusts their coordination to octahedral geometry at the surface of nanocrystallites and changes the electronic properties of TiO_2. In such hybrid structures localized orbitals of surface-attached ligands, are electronically coupled with the delocalized electron levels from the conduction band of a TiO_2 semiconductor [16]. As a consequence, absorption of light by the charge–transfer (CT) complex yields to the excitation of electrons from the chelating ligand directly into the conduction band of TiO_2 nanocrystallites. This results in a red shift of the semiconductor absorption compared to that of unmodified nanocrystallites and enables efficient harvesting of solar photons. Additionally, this type of electronic coupling yields to instantaneous separation of photogenerated charges into two phases, the holes localize on the donating organic modifier, and the electrons delocalize in the conduction band of TiO_2. Moreover, the enediol ligands were found to act as conductive leads, allowing wiring of oligonucleotides and proteins resulting in enhanced charge separation and ensuing chemical transformations [17, 18].

In last two decades the surface modification of commercial TiO_2 (Degussa P25, $d = 30$ nm) with benzene derivatives (mainly catechol and salicylic acid) was studied [19–34]. Just few articles [9, 13–15, 35] investigated CT complex formation between enediol ligands and colloidal TiO_2 nanoparticles ($d = 45$ Å), where binding of modifiers is stabilized by ligand-induced surface reconstruction of the nanoparticles.

Herein, we report surface modification of TiO_2 nanoparticles with enediol ligands (catechol, pyrogallol, and gallic acid) that are able to adjust the coordination geometry of the surface Ti atoms inducing shift of the absorption onset toward the visible region of the spectrum, compared to unmodified nanocrystallites. Since these novel CT semiconducting materials exhibit optical properties that are distinct from their constituents, not absorbing in the visible region, Benesi–Hildebrand analysis for molecular complexes was employed to determine the stability constants from the absorption spectra. The stoichiometry of formed complexes was obtained using Job's method of continuous variation. The binding structures were investigated by using FTIR spectroscopy.

Experimental Section

All the chemicals were of the highest purity available and were used without further purification (Aldrich, Fluka). Milli-Q deionized water (resistivity 18.2 MΩ cm^{-1}) was used as solvent. The colloidal TiO_2 dispersions were prepared by the dropwise addition of titanium(IV) chloride to cooled water. The pH of the solution was between 0 and 1, depending on the $TiCl_4$ concentration. Slow growth of the particles was achieved by using dialysis at 4 °C against water until the pH = 3.5 was reached [36]. The concentration of TiO_2 (0.2 M) was determined from the concentration of the peroxide complex obtained after dissolving the colloid in concentrated H_2SO_4 [37]. The mean particle diameter of titania used in this study was 45 Å.

Surface modification of TiO_2 resulting in the formation of a CT complex was achieved by the addition of surface-active ligands up to concentrations required to cover all surface sites ($[Ti_{surf}] = [TiO_2]12.5/D$ [38], where Ti_{surf} is the molar concentration of surface Ti sites, $[TiO_2]$ is the molar concentration of TiO_2 in molecular units, and D is the diameter of the particle in angstroms). As the consequence of enhanced particle–particle interaction, upon surface modification that eliminates the surface charge, precipitation, and/or "gelling" of the solution may occur. In order to avoid these problems pH of the solution was adjusted to 2 with HCl. For the determination of CT complex binding constants the absorption spectra were recorded at room temperature in cells with 1 cm optical path length using Thermo Scientific Evolution 600 UV/Vis spectrophotometer. The experiments determining the composition of complexes by Job's method [39] were conducted by using 7.2 mM TiO_2 and 2 mM modifier solutions. Nine mixtures of TiO_2 and modifier were prepared—volumes of TiO_2 solution used varied from 1 to 9 mL and those of modifiers' solutions from 9 to 1 mL; and total volume was always 10 mL.

Infrared spectra were taken in attenuated total reflection (ATR) mode using a Nicolet 380 FTIR spectrometer equipped with a Smart Orbit™ ATR attachment containing a single-reflection diamond crystal. The angle of incidence was 45°. In order to avoid the precipitation of modified TiO_2 and the excess of unbound modifier, in the preparation of samples for FTIR measurements the quantity of ligands added was 50% of all Ti_{surf} sites ($[TiO_2] = 0.2$ M, $c_{LIGAND} = 25$ mM). The dispersions containing surface modified TiO_2 nanoparticles were dried under argon at room temperature, and powders obtained were placed into the vacuum oven for 8 h to get to complete dryness. Before

measuring FTIR spectra, powders were triturated in the agate mortar. Typically, 64 scans were performed for each spectrum with 4 cm^{-1} resolution. The spectrum of the dried TiO_2 aqueous slurry (not containing modifier) was used as the background.

Results and Discussion

Optical Properties of Surface Modified Nanocrystalline TiO_2

When TiO_2 particles are in the nanocrystalline regime, a large fraction of the atoms that constitute the nanoparticle is located at the surface with significantly altered electrochemical properties. As the size of nanocrystalline TiO_2 becomes smaller than 20 nm the surface Ti atoms adjust their coordination environment from hexacoordinated (octahedral) to pentacoordinated (square pyramidal), which is followed by the compression of the Ti–O bond to accommodate for the curvature of the nanoparticle [10]. These undercoordinated defect sites are the source of novel enhanced and selective reactivity of nanoparticles toward bidentate ligand binding. All of the investigated ligands listed in Table 1 were found to undergo binding at the surface (see inset in Fig. 1), inducing new hybrid properties of the surface-modified nanoparticle colloids. These hybrid properties arise from the ligand-to-metal CT interaction coupled with electronic properties of the core of semiconductor nanoparticles.

Consequently, the onset of absorption of these CT nanocrystallites is red shifted compared to unmodified TiO_2 (Fig. 1). The shift in the absorption edge in the modified semiconductor nanoparticles is attributed to the excitation of localized electrons from the surface modifier into the conduction band continuum states of the semiconductor particle [13]. Similar position of the absorption threshold for surface-modified nanoparticles with catechol, pyrogallol, and gallic acid (bandgaps are presented in Table 1) is probably the consequence of very similar dipole moments of various surface bound Ti–ligand complexes formed [9].

Apart from the shift in the absorption edge, the optical properties of surface modified semiconductor nanoparticles, having a continuous rise of absorption toward higher energies, paralleled the absorption properties characteristic of the band structure in bare semiconductor nanoparticles. A similar red shift, but in localized CT complex resulting in a pronounced absorption maximum, was previously observed for Ti^{4+} and catechol [40], salicylic [41], or ascorbic acid [42].

It should be noted that all investigated enediol ligands are by themselves extremely susceptible to oxidation. Apparently, because of the bidentate binding to nanoparticles, enediol ligands gain stability and are not easily oxidized. Enediol-modified TiO_2 colloids preserved their optical properties even after exposure to daylight for 2–3 months.

Due to the existence of undercoordinated surface defect sites and their lower efficiency of covalent bonding with solvent molecules in comparison with covalent bonding between atoms within the TiO_2 lattice, the surface species posses energy level in the midgap region [43]. Apart from red shift of the absorption onset of surface modified TiO_2 nanoparticles, CT interaction between the molecule of modifier and surface Ti atoms also induces fine-tuning of

Table 1 Ligands used for modification of TiO_2 nanoparticles, Benesi–Hildebrand binding constants, and bandgaps upon binding

Ligand	Structural formula	K_b (M^{-1})[a]	Bandgap (eV)
Catechol	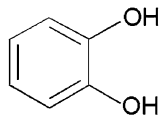	2490 ± 120	1.96
Pyrogallol	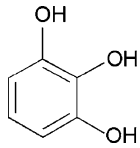	3130 ± 120	1.89
Gallic acid	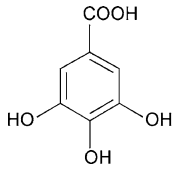	1700 ± 100	1.92

[a] The absorption wavelengths at which the stability constants were determined are 400 nm (catechol), 475 nm (gallic acid), and 425 nm (pyrogallol)

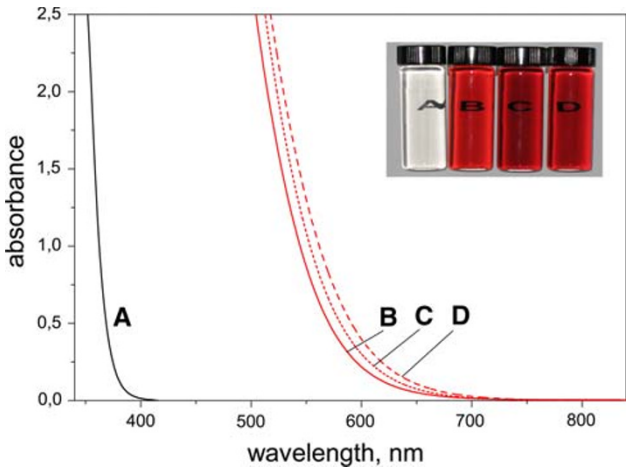

Fig. 1 Absorption spectra of surface modified 45 Å TiO_2 nanoparticles (0.09 M, pH 2) with different ligands (2.5 mM): (*A*) bare TiO_2; (*B*) catechol; (*C*) gallic acid; and (*D*) pyrogallol. Molecular structures of ligands are shown in Table 1

the electrochemical potential of semiconductor nanocrystals indicating changes in oxidizing abilities.

Upon surface modification, the effective bandgap of catechol-, gallic acid-, and pyrogallol-modified TiO_2 nanoparticles at pH = 2 were determined to be: 1.96, 1.92, and 1.89 eV, respectively. These results indicate similar electrochemical potentials of semiconducting nanocrystals modified with chosen class of enediol ligands indicating similar binding structures and effective electronic coupling. TiO_2 nanoparticles modified with this type of bidentate benzene derivatives can be used for development of Type II dye-sensitized nanoporous titania solar cells where the dyes bind to the particle surface through enediol groups [44]. Also, blends of surface modified TiO_2 nanoparticles and organic semiconductors cast from co-solutions can be used for synthesis of hybrid solar cells combining the unique properties of inorganic semiconductor and film-forming properties of polymers [45].

Determination of Stability (Binding) Constants

Since these novel CT semiconducting materials exhibit optical properties that are distinct from their constituents, not absorbing in the visible region, Benesi–Hildebrand analysis for molecular complexes [46, 47] can be employed to determine the stability constant of CT complex. Benesi–Hildebrand analysis can be used for small particles since the same relationship is obtained between the stability constant and ligand concentration from Langmuir isotherm used for bulk compounds [9]. For a colloidal solution of 45 Å TiO_2 one can consider the formation of an inner-sphere CT complex

$$\mathrm{Ti_{surf}} + \mathrm{L} \leftrightarrows \mathrm{CT_{complex}} \quad (1)$$

with the stability constant K_b expressed as

$$K_b = \frac{[\mathrm{CT_{complex}}]_{eq}}{[\mathrm{Ti_{surf}}]_{eq}[\mathrm{L}]_{eq}} \quad (2)$$

Since the absorption in the visible region originates solely from the complex formed it is obvious that $[\mathrm{CT_{complex}}] = A/\varepsilon l$ and the Eq. 2 can be rearranged to the following linearized form

$$\frac{1}{A} = \frac{1}{K_b A_{max}} \frac{1}{[L]} + \frac{1}{A_{max}} \quad (3)$$

where [L] is the concentration of ligand, A and A_{max} the absorbances of a CT complex for a given concentration of ligand L, and saturation concentration corresponding to the full coverage of TiO_2 surface, respectively.

Stability constants K_b were determined from the absorbances of a series of solutions (Fig. 2) containing a fixed concentration of TiO_2 nanoparticles (c_{TiO_2} = 3.5 mM, i.e., 0.97 mM Ti_{surf} according to equation in "Experimental" section) and increasing concentrations of ligands (c_{ligand} = 0.06–1.23 mM). In order to avoid great errors in K_b determination, the wavelength of complex absorption is chosen for each ligand to correspond to the requested absorption range ($0.1 < A < 0.9$) [47]. By plotting $1/A$ vs. 1/[L] the straight lines were obtained and from the ratio of the intercept and the slope, K_b were determined and presented in Table 1. From the molecular structures of ligands used it can be concluded that two types of binding to Ti_{surf} may appear—catecholate type (OH, OH) or carboxylate (COOH) in the case of gallic acid solely. However, it is quite obvious that by comparing the measured values of K_b one cannot differentiate between these two types of binding since these values are similar, of the order 10^3 M^{-1}. In the literature, to determine the CT complex stability constants for catechol and/or gallic acid the adsorption approach after filtration method [14, 20, 21, 28] or FTIR measurements [29, 30] have been used and two to three times larger K_b values were reported. We believe that lower K_b values we reported are more precisely determined since they are obtained from the absorbance measurements directly.

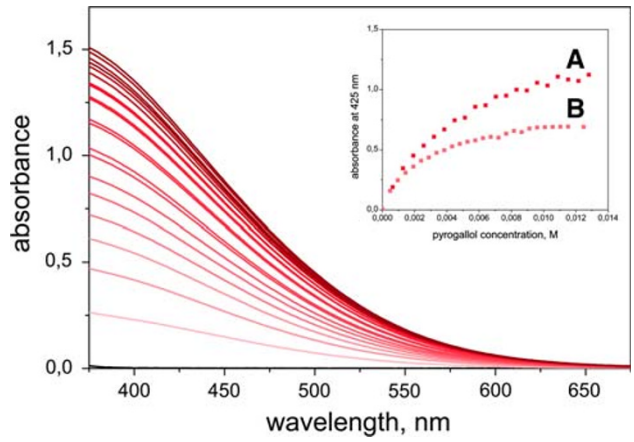

Fig. 2 Absorption spectra of 3.5 mM TiO_2 nanoparticles before and after surface modification with pyrogallol (0–1.23 mM in 0.06 mM steps). Inset: Absorption at 425 nm of TiO_2–pyrogallol CT complex versus pyrogallol concentration (data recorded 20 h after surface modification). Solutions of TiO_2 nanoparticles used for modification were freshly prepared (*A*) and 4-years-old (*B*)

It must be pointed out that very interesting phenomenon was observed when TiO_2 solutions of the same molecular concentration (3.5 mM) freshly prepared and 4-years-old were used for modification (Inset of Fig. 2). A_{425} versus pyrogallol concentration curve for freshly prepared TiO_2 shows much higher saturation value of A_{425} than was observed in the case of 4-years-old TiO_2 colloidal solution ($A_{425}^{\text{4-years aged}} = 0.65\ A_{425}^{\text{fleshly prepared}}$). It is known that crystallinity increases with aging of TiO_2 nanoparticles inducing the decrease in concentration of coordinatively

unsaturated surface defect sites. In order to eliminate the possibility that decrease in number of Ti_{surf} sites is simply the consequence of agglomeration or Oswald ripening we performed the measurements of the particle size diameter using dynamic light scattering (DLS). In both cases (freshly prepared and 4-years-old TiO_2 solutions) the effective diameter was found to be the same.

Additionally, the stoichiometric ratio between Ti_{surf} atoms and modifiers in the CT complexes was checked by Job's method of continuous variation [39] assuming that only one type of complex is present in solution. The results obtained for catechol and gallic acid are presented in Fig. 3. Job's plots for both complexes reached a maximum value at a mole fraction of $[Ti_{surf}]/[Ti_{surf}] + [L] = 0.7$, confirming that molar ratio between Ti_{surf} atoms and ligands in the complex is 2:1. The same Ti_{surf}/ligand molar ratio was obtained for pyrogallol.

Binding Structure of Ligands at Nanoparticle Surface

The way ligands bind to TiO_2 surface was investigated by using ATR–FTIR spectroscopy. Since the infrared spectrum of dried TiO_2 has only the characteristic broadband in 3700–2000 cm^{-1} region [9], we were able to measure spectra of modified colloids in 1750–1000 cm^{-1} region where the characteristic bands of modifiers exist. Spectra of adsorbed ligands were obtained by subtracting the spectrum of bare TiO_2 nanoparticles from the spectrum of surface modified TiO_2 nanoparticles.

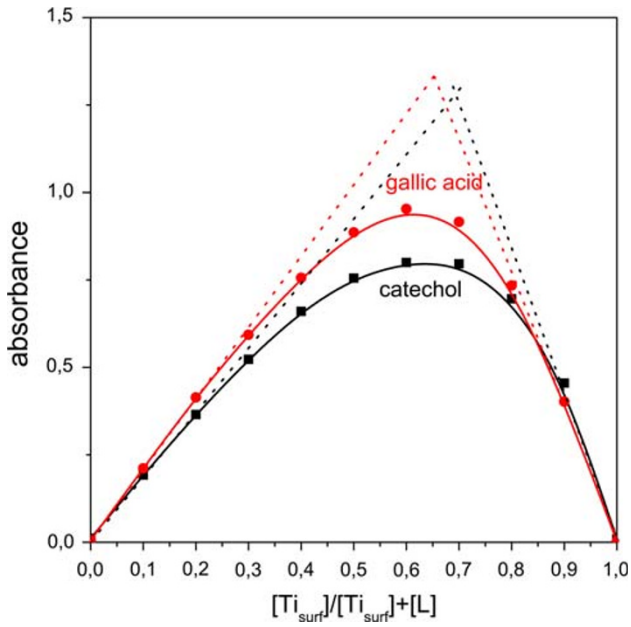

Fig. 3 Job's curve of equimolar solutions for ligand–Ti_{surf} complex ($A_{catechol}$, at 400 nm; $A_{gallic\ acid}$ at 475 nm); $[Ti_{surf}] + [L] = 2$ mM

The ATR–FTIR spectra of catechol, free and adsorbed on TiO_2 nanoparticles were presented in Fig. 4. The main bands and their assignments [29, 30, 34] in free catechol (curve A) are as follows: stretching vibrations of the aromatic ring ν(C–C)/ν(C=C) at 1618, 1594, 1512, and 1468 cm^{-1}, stretching vibrations of the phenolic group ν(C–OH) at 1279, 1254 and 1239 cm^{-1}, bending vibrations of the phenolic group δ(C–OH) at 1365, 1184, 1163, and 1149 cm^{-1} and bending δ(C–H) at 1039 and 1093 cm^{-1}. Upon adsorption of catechol onto TiO_2 (curve B) the difference between FTIR spectra of free and adsorbed modifier appears, indicating surface complexation with catechol bound to the oxide surface in bidentate form [29, 30]. Bending δ(C–OH) vibrations in the region below 1200 cm^{-1} loose their hyperfine structure, while the pronounced band at 1365 cm^{-1} nearly disappears and a very weak and broad feature centered at 1354 cm^{-1} appears. Three bands of stretching vibrations ν(C–OH) merge to one prominent band at 1249 cm^{-1}. The binding of catechol to TiO_2 via two adjacent phenolic groups even affects the stretching of the aromatic ring (bands above 1400 cm^{-1}).

Catecholate type of binding inherent to catechol molecule adsorption to metal-oxide surfaces, with two adjacent phenolic OH groups taking part in complexation, was reported to result in the formation of both bidentate mononuclear chelating and/or bidentate binuclear bridging complexes. There are two opinions dealing with catecholate binding: some authors [9, 48, 49] claim that five-membered ring coordination complexes predominate, while the others [16, 20, 21, 29, 30] find bridging complexes energetically more favorable. Since according to Job's curve the molar ratio between Ti_{surf} atoms and

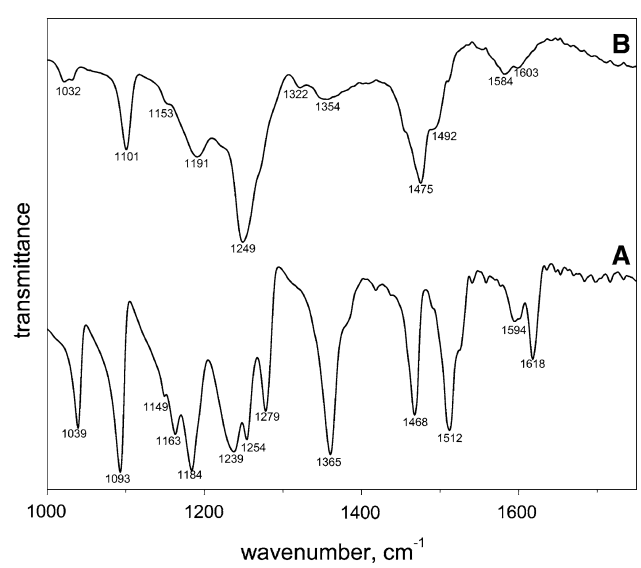

Fig. 4 FTIR spectra of catechol: free (*A*) and adsorbed on TiO_2 nanoparticles (*B*)

catechol in the complex is 2:1 (Fig. 3), the CT complex formed is most likely bidentate binuclear (bridging) complex (Scheme 1).

The ATR–FTIR spectra of pyrogallol, free and adsorbed on TiO_2 nanoparticles were presented in Fig. 5. The main bands and their assignments [50] in free pyrogallol (curve A) are as follows: stretching vibrations of the aromatic ring ν(C–C)/ν(C=C) at 1619, 1518, 1479, 1402, and 1383 cm^{-1}, stretching vibrations of the phenolic group ν(C–OH) at 1518, 1402, 1315, 1285, 1242, and 999 cm^{-1}, bending vibrations of the phenolic group δ(C–OH) at 1479, 1383, 1350, 1189, and 1156 cm^{-1} and bending δ(C–H) at 1150 and 1064 cm^{-1}. The adsorption of pyrogallol onto TiO_2 nanoparticles (curve B) leads to obvious changes in FTIR spectra: complete disappearance of the bands at 1518, 1402, 1383, 1350, and 1285 cm^{-1}, shift of the band at 999 to 1032 cm^{-1}, and the intensity attenuation of the bands at 1315, 1189, and 1156 cm^{-1}. The results obtained are quite expected since these bands are assigned to stretching and bending vibrations of phenolic OH groups that participate in the formation of CT complex with Ti surface atoms. The binding of pyrogallol to TiO_2, like in the case of catechol, also shifts the bands assigned to stretching of the aromatic ring in the region above 1400 cm^{-1}. Bands at 1315, 1242, 1189, and 1157 cm^{-1}, being changed in intensity, are probably the vibrations of the unbound, third phenolic OH group of pyrogallol, since just two adjacent phenolic groups participate in binding (Scheme 1).

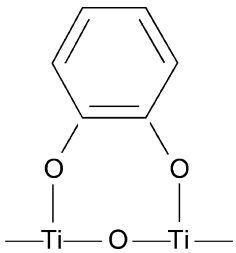

Scheme 1 Coordination mode of Ti_{surf}–catechol complex

The ATR–FTIR spectra of gallic acid, free and adsorbed on TiO_2 nanoparticles were presented in Fig. 6. The main bands and their assignments [30, 50] in free protonated gallic acid (curve A) are as follows: stretching vibrations of the aromatic ring ν(C–C)/ν(C=C) at 1612, 1539, 1469, and 1437 cm^{-1}, stretching vibrations of the phenolic group ν(C–OH) at 1372, 1305, 1240, and 1020 cm^{-1}, bending vibrations of the phenolic group δ(C–OH) at 1336, 1240, and 1100 cm^{-1}, stretching and/or bending vibrations of CO or OH in COOH at 1199, 1100, and 1046 cm^{-1} and pronounced stretching vibration of the carbonyl group ν(C=O) at 1698 cm^{-1}. The adsorption of gallic acid onto TiO_2 nanoparticles (curve B) leads to complete disappearance of the bands at 1372 and 1305 cm^{-1}, while the band at 1020 cm^{-1} disappears with the formation of broad intensive band at 1070 cm^{-1}. The band at 1240 cm^{-1}, although slightly shifted, is preserved with decreased intensity. These bands, assigned to stretching and bending vibrations of phenolic OH groups (ν(C–OH) and δ(C–OH)), are probably those participating in the formation of CT complex with Ti surface atoms. Since upon binding the third phenolic group remains unbound, bands at 1336 and 1240 cm^{-1} remain in spectrum, although slightly shifted and with decreased intensity. The pronounced bands assigned to the vibrations of the carboxylic group (1199 and 1698 cm^{-1}) remain in the spectrum suggesting that this group is not involved in complexation. The binding of

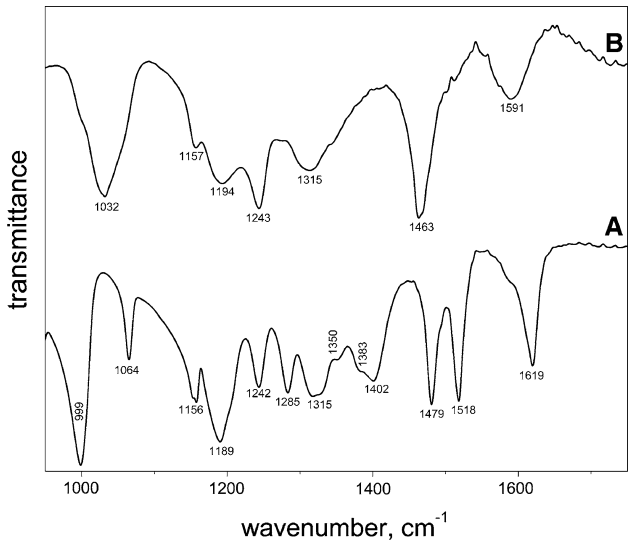

Fig. 5 FTIR spectra of pyrogallol: free (*A*) and adsorbed on TiO_2 nanoparticles (*B*)

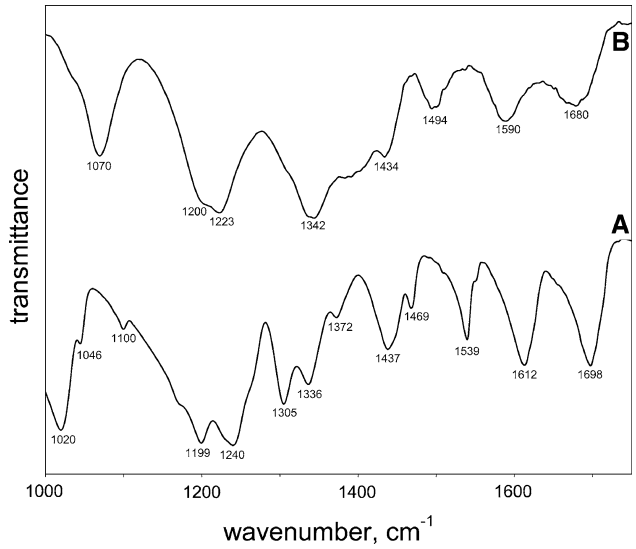

Fig. 6 FTIR spectra of gallic acid: free (*A*) and adsorbed on TiO_2 nanoparticles (*B*)

gallic acid to TiO_2, like in the case of catechol and pyrogallol, also shifts the bands assigned to stretching of the aromatic ring in the region above 1400 cm^{-1}.

According to the molecular structure of gallic acid two types of binding to Ti_{surf} may appear—catecholate (OH, OH) or carboxylate (COOH) type. Literature data are quite controversial whether or not benzoic acid, having only COOH functional group, adsorbs on TiO_2 surface. Tunesi and Anderson [19, 22] claim that no adsorption was observed, while the others [14, 16, 31, 33, 51] confirmed the formation of bidentate chelate or bridging complexes, pointing out weak adsorption [14, 31]. According to FTIR results obtained we may conclude that in the case of gallic acid binding through carboxylate group does not exist. Possible reason for that is as follows: in the carboxylate type of binding formation of chelated four-membered ring is proposed [32] being energetically less favorable than the ring formed through catecholate group (Scheme 1).

Hence, in all three ligands investigated (catechol, pyrogallol, and gallic acid) catecholate type of binding is obvious, since carboxylate type of binding takes no part in the binding of gallic acid to TiO_2 nanoparticles.

Conclusions

All investigated ligands (catechol, pyrogallol, and gallic acid) form inner-sphere CT complexes with TiO_2 nanoparticles ($d = 45$ Å). Binding of the modifier molecules to undercoordinated surface Ti atoms (defect sites) results in a significant change in the onset of absorption and the effective bandgap. From the Benesi–Hildebrand plot, the stability constants at pH 2 of the order 10^3 M^{-1} have been determined. For chosen enediol modifiers binding was found to be through bidentate binuclear (bridging) complexes leading to restoration of six-coordinated octahedral geometry of surface Ti atoms. Stabilized charge separation, being important feature of these systems opens-up possibility for using modifier molecules as conductive leads that allow electronic linking of the nanoparticle into molecular circuits providing further extension of photoinduced electron transfer.

Acknowledgment Financial support for this study was granted by the Ministry of Science and Technological Development of the Republic of Serbia (Project 142066).

References

1. A. Hagfeldt, M. Grätzel, Chem. Rev. **95**, 49 (1995). doi:10.1021/cr00033a003
2. M. Grätzel, Nature **414**, 338 (2001). doi:10.1038/35104607
3. B. O'Regan, M. Grätzel, Nature **353**, 737 (1991). doi:10.1038/353737a0
4. A.J. Nozik, Annu. Rev. Phys. Chem. **29**, 189 (1978). doi:10.1146/annurev.pc.29.100178.001201
5. X. Fu, W.A. Zeltner, M.A. Anderson, Appl. Catal. B Environ. **6**, 209 (1995). doi:10.1016/0926-3373(95)00017-8
6. D. Bahnemann, Sol. Energy **77**, 445 (2004). doi:10.1016/j.solener.2004.03.031
7. Y. Kikuchi, K. Sanada, T. Iyoda, K. Hashimoto, A. Fujishima, J. Photochem. Photobiol. Chem. **106**, 51 (1997). doi:10.1016/S1010-6030(97)00038-5
8. Z.V. Šaponjić, N.M. Dimitrijević, D.M. Tiede, J.A. Goshe, X. Zuo, L.X. Chen, A.S. Barnard, P. Zapol, L. Curtiss, T. Rajh, Adv. Mater. **17**, 965 (2005). doi:10.1002/adma.200401041
9. T. Rajh, L.X. Chen, K. Lukas, T. Liu, M.C. Thurnauer, D.M. Tiede, J. Phys. Chem. B **106**, 10543 (2002). doi:10.1021/jp021235v
10. L.X. Chen, T. Rajh, W. Jäger, J. Nedeljkovic, M.C. Thurnauer, J. Synchrotron. Radiat. **6**, 445 (1999). doi:10.1107/S090904959801591X
11. F. Farges Jr., G.E. Brown, J.J. Rehr, Geochim. Cosmochim. Acta. **60**, 3023 (1996). doi:10.1016/0016-7037(96)00144-5
12. N.M. Dimitrijević, Z.V. Šaponjić, D.M. Bartels, M.C. Thurnauer, D.M. Tiede, T. Rajh, J. Phys. Chem. B **107**, 7368 (2003). doi:10.1021/jp034064i
13. T. Rajh, J.M. Nedeljković, L.X. Chen, O. Poluektov, M.C. Thurnauer, J. Phys. Chem. B **103**, 3515 (1999). doi:10.1021/jp9901904
14. J. Moser, S. Punchihewa, P.P. Infelta, M. Grätzel, Langmuir **7**, 3012 (1991). doi:10.1021/la00060a018
15. T. Rajh, D.M. Tiede, M.C. Thurnauer, J. Non-Cryst. Solid **205-207**, 815 (1996)
16. P. Persson, R. Bergström, S. Lunell, J. Phys. Chem. B **104**, 10348 (2000). doi:10.1021/jp002550p
17. T. Rajh, Z. Šaponjić, J. Liu, N.M. Dimitrijević, N.F. Scherer, M. Vega-Arroyo, P. Zapol, L.A. Curtiss, M.C. Thurnauer, Nano Lett. **4**, 1017 (2004). doi:10.1021/nl049684p
18. N.M. Dimitrijević, Z.V. Šaponjić, B.M. Rabatić, T. Rajh, J. Am. Chem. Soc. **127**, 1344 (2005). doi:10.1021/ja0458118
19. S. Tunesi, M. Anderson, J. Phys. Chem. **95**, 3399 (1991). doi:10.1021/j100161a078
20. S.T. Martin, J.M. Kesselman, D.S. Park, N.S. Lewis, M.R. Hoffman, Environ. Sci. Technol. **30**, 2535 (1996). doi:10.1021/es950872e
21. P. Rodriguez, M.A. Blesa, A.E. Regazzoni, J. Colloid Interface Sci. **177**, 122 (1996). doi:10.1006/jcis.1996.0012
22. A.E. Regazzoni, P. Mandelbaum, M. Matsuyoshi, S. Schiller, S.A. Bilmes, M.A. Blesa, Langmuir **14**, 868 (1998). doi:10.1021/la970665n
23. Y. Liu, J.I. Dadap, D. Zimdars, K.B. Eisenthal, J. Phys. Chem. B **103**, 2480 (1999). doi:10.1021/jp984288e
24. D. Robert, S. Parra, C. Pulgarin, A. Krzton, J.V. Weber, Appl. Surf. Sci. **167**, 51 (2000). doi:10.1016/S0169-4332(00)00496-7
25. A.D. Roddick-Lanzilotta, A.J. McQuillan, J. Colloid Interface Sci. **227**, 48 (2000). doi:10.1006/jcis.2000.6864
26. A.D. Weisz, A.E. Regazzoni, M.A. Blesa, Solid State Ion **143**, 125 (2001). doi:10.1016/S0167-2738(01)00840-2
27. A.D. Weisz, L. Garcia Rodenas, P.J. Morando, A.E. Regazzoni, M.A. Blesa, Catal. Today **76**, 103 (2002). doi:10.1016/S0920-5861(02)00210-9
28. D.V. Heyd, B. Au, J. Photochem. Photobiol. A Chem. **174**, 62 (2005). doi:10.1016/j.jphotochem.2005.03.009
29. P.Z. Araujo, C.B. Mendive, L.A. Garcia Rodenas, P.J. Morando, A.E. Regazzoni, M.A. Blesa, D. Bahnemann, Colloid Surf. A **265**, 73 (2005). doi:10.1016/j.colsurfa.2004.10.137

30. P.Z. Araujo, P.J. Morando, M.A. Blesa, Langmuir **21**, 3470 (2005). doi:10.1021/la0476985
31. A.M. Johnson, S. Trakhtenberg, A.S. Cannon, J.C. Warner, J. Phys. Chem. A **111**, 8139 (2007). doi:10.1021/jp071398p
32. S. Tunesi, M.A. Anderson, Langmuir **8**, 487 (1992). doi:10.1021/la00038a030
33. K.D. Dobson, A.J. McQuillan, Spectrochim. Acta [A] **56**, 557 (2000). doi:10.1016/S1386-1425(99)00154-7
34. P.A. Connor, K.D. Dobson, A.J. McQuillan, Langmuir **11**, 4193 (1995). doi:10.1021/la00011a003
35. N.M. Dimitrijević, O.G. Poluektov, Z.V. Šaponjić, T. Rajh, J. Phys. Chem. B **110**, 25392 (2006). doi:10.1021/jp064469d
36. T. Rajh, A.E. Ostafin, O.I. Micic, D.M. Tiede, M.C. Thurnauer, J. Phys. Chem. **100**, 4538 (1996). doi:10.1021/jp952002p
37. G.M. Eisenberg, Ind. Eng. Chem. Anal. **15**, 327 (1943). doi:10.1021/i560117a011
38. L.X. Chen, T. Rajh, Z. Wang, M.C. Thurnauer, J. Phys. Chem. B **101**, 10688 (1997). doi:10.1021/jp971930g
39. W.C. Vosburgh, G.R. Copper, J. Am. Chem. Soc. **63**, 437 (1941). doi:10.1021/ja01847a025
40. B.A. Borgias, S.R. Cooper, Y.B. Koh, K.N. Raymond, Inorg. Chem. **23**, 1009 (1984). doi:10.1021/ic00176a005
41. A.E. Hultquist, Anal. Chem. **36**, 149 (1964). doi:10.1021/ac60207a048
42. E.D. Hines, F. Boltz, Anal. Chem. **24**, 947 (1952). doi:10.1021/ac60066a007
43. N. Serpone, E. Pelizzetti, *Photocatalysis. Fundamentals and application* (Wiley Interscience, New York, 1989)
44. E.L. Tae, S.H. Lee, J.K. Lee, S.S. Yoo, E.J. Kang, K.B. Yoon, J. Phys. Chem. B **109**, 22513 (2005). doi:10.1021/jp0537411
45. S. Günes, N. Marjanović, J.M. Nedeljković, N.S. Sariciftci, Nanotechnology **19**, 424009 (2008). doi:10.1088/0957-4484/19/42/424009
46. H.A. Benesi, J.H. Hildebrand, J. Am. Chem. Soc. **71**, 2703 (1949). doi:10.1021/ja01176a030
47. W.B. Person, J. Am. Chem. Soc. **87**, 167 (1965). doi:10.1021/ja01080a006
48. M. Vega-Arroyo, P.R. Le Breton, T. Rajh, P. Zapol, L.A. Curtiss, Chem. Phys. Lett. **406**, 306 (2005). doi:10.1016/j.cplett.2005.03.029
49. P.C. Redfern, P. Zapol, L.A. Curtiss, T. Rajh, M.C. Thurnauer, J. Phys. Chem. B **107**, 11419 (2003). doi:10.1021/jp0303669
50. I. Mohammed-Ziegler, F. Billes, J. Mol. Struct. (Theochem.) **618**, 259 (2002). doi:10.1016/S0166-1280(02)00547-X
51. K.S. Finnie, J.R. Bartlett, J.L. Woolfrey, Langmuir **14**, 2744 (1998). doi:10.1021/la971060u